Transaction A: Civil Engineering
Vol. 17, No. 4, pp. 245–261

Dynamic Properties of Gravelly Materials

A. Aghaei Araei[1,*], H.R. Razeghi[1], S. Hashemi Tabatabaei[2] and A. Ghalandarzadeh[3]

Abstract. *This paper studies the dynamic characteristics (i.e. shear modulus and damping ratio) of modeled gravelly soils used as construction materials in some rock-fill dams in Iran by conducting large-scale triaxial testing. Tested specimens were compacted to more than 95% maximum dry density, according to Modified Proctor, and tested according to ASTM D 3999. Accurate monitoring of strains by means of non-contact type displacement transducers to infinitesimal strains as small as 0.0001% enabled us to obtain $G_{\max}$ with some extrapolation. Based on the available experimental results the ranges for $G/G_{\max} - \gamma$ and $D - \gamma$ are defined for materials with $>$ 30% fine content and materials with $<$ 15% fine content. The results clearly indicate the need for modification in previously proposed $G/G_{\max} - \gamma$ curves, particularly for gravels with $>$ 30% fine content. Also, the suggested $D - \gamma$ curves lay out of the bounds of data reported by previous researchers, which may be due to the effects of testing frequency, fine content, and confining pressure. In addition, a predictive hyperbolic model for estimating normalized shear modulus ($G/G_{\max}$) versus shear strain (γ) is presented. Effects of the number of cyclic loadings over the shear modulus and damping ratio are also investigated.*

Keywords: *Rock-fill; Triaxial testing; Shear modulus; Damping; Excess pore pressure.*

INTRODUCTION

The seismic design of earth and rock-fill dams with a clay core in earthquake prone regions requires determination of the dynamic characteristics of the used materials. The most important dynamic parameters of soils in any equivalent linear analyses are shear modulus (G) and damping ratio (D). For most soils, at very low shear strain levels (less than 0.0001%), the shear modulus and damping ratio are essentially constant for a given frequency, and the shear modulus is at its maximum value, $G_{\max}$. The plot of $G/G_{\max}$ versus γ is called a normalized modulus reduction curve. Almost no $G - \gamma$ and $D - \gamma$ relationships were available for gravels until Seed et al. [1] who published results from a large diameter ($\approx$ 300 mm) cyclic triaxial shear test on four rock-fill dam materials. Over the two past decades, however, results have been become available from many investigators [2-10], which were limited to tests performed at a loading frequency less than 0.2 Hz.

This paper presents the results of large scale triaxial tests on modeled gravelly materials used for construction in six earth and rock-fill dams in Iran. The present study mainly focuses on:

1. Presenting a series of curves for shear modulus and damping ratio versus shear strain relationships.
2. Reviewing the factors, such as fine content, loading frequency, confining pressure, number of cyclic loadings and excess pore pressure generation, which may affect these parameters, developing predictive equations for estimation of the normalized shear modulus and material damping ratio.

PREVIOUS STUDIES ON PARAMETRIC CHARACTERISTICS OF GRAVELLY SOILS

Seed and Idriss [11] observed the relationship between G, σ'_3, void ratio (e) and shear strain (γ) using laboratory cyclic triaxial testing. They found that the value of G at small strains ($G_{\max}$) is variable, between

1. *School of Civil Engineering, Iran University of Science and Technology (IUST), Narmak, Tehran, P.O. Box 16765-163, Iran.*
2. *Department of Geotechnical Engineering, Building and Housing Research Center (BHRC), Tehran, P.O. Box 13145-1696, Iran.*
3. *Department of Civil Engineering, University of Tehran, Tehran, P.O. Box 11365-4563, Iran.*
*. *Corresponding author. E-mail: aaghaee@iust.ac.ir*

Received 13 May 2009; received in revised form 18 April 2010; accepted 14 June 2010

93.3 to 233.3 MPa for sands, and $G_{\max}$ increases with void ratio decrease. Seed et al. [1] expanded the Seed and Idriss [11] study by performing cyclic triaxial tests on 30 cm diameter over reconstituted specimens of four rock-fill dam materials. Testing conditions were: $D_r = 60 - 95\%$, confining pressure = 200 kPa, loading frequency = 0.017 Hz, number of cycles-measure/total = 5/6, and drainage condition= saturated/un-drained. The results demonstrated that $G_{\max}$ is significantly higher for gravels and ranges between 248.8 and 560 MPa. They noted that for gravels:

1. The value of G decreases markedly as the cyclic shear strain increases.
2. The value of G increases with an increase in the relative density.
3. The stronger rock-fill materials have higher G values.
4. The grain size distribution does not appear to be a significant factor for determination of shear modulus.

It is common to use normalized modulus reduction ($G/G_{\max}$) versus γ relationships. The main values of curves defining $G/G_{\max}$ versus γ for gravels are typically 10-30% less than those for sands [11]. However, there is a slight overlapping in the range for sands and gravels.

In order to define the mean normalized shear modulus, $G/G_{\max}$, versus cyclic shear strain, γ, Rollins et al. [7] employed a hyperbolic model for gravels based on data from 15 investigators. The acquired mean curve for gravels was somewhat different from the results reported by Seed et al. [1]. Essentially, Rollins et al. [7] results were obtained under the following conditions: sample type = reconstituted and undisturbed; ranges of confining pressures= 29-490 kPa; density of samples = 27-95%; loading frequency = 0.01-0.2 Hz; number of total cycles = 3-12; maximum grain size = 10-150 mm, and fine contents = 0%-9% (average = 5%). They found that the $G/G_{\max}$ versus γ curve is essentially independent of sample disturbance, fines content (range 0-9%), gravel content and relative density. However, it is moderately dependent on confining pressure.

The materials damping ratio (D) represents the energy dissipated by the soils. Mechanisms contributing to material damping are: friction between soil particles, viscosity of the soil skeleton and viscosity of the pore fluid. Theoretically, there should be no dissipation of energy in the linear elastic range ($G_{\max}$) for the hysteretic damping model. However, even at very low strain levels, there is always some energy dissipation measured in laboratory specimens due to visco-elastic behavior [12]. The damping ratio at very low strain levels is a constant value and is referred to as the small strain damping ratio ($D_{\min}$). At higher strains, nonlinearity in the stress-strain relationship leads to an increase in material damping ratio with increasing strain amplitude. It might be expected that dense materials would dissipate more energy and hence have a higher damping ratio than loose materials. Thus, with increasing density, the damping ratio increases slightly in cohesionless materials [11]. Modulus attenuation curves (damping ratio) for most cohesionless soils (sands and gravels) are very similar and not significantly dependent on the grain size (i.e. fine content and gravel content) of the particles [1,11].

Rollins et al. [7] introduced a hyperbolic model for the D versus γ relationship in gravels, claiming that the relationship is independent of sample disturbance, yet moderately dependent on confining pressure.

Darendeli [13] and Stokoe et al. [14] developed a method to attain D from $G/G_{\max}$ for sands, silts and clays. Zhang et al. [9] adopted the mentioned approach to estimate D from $G/G_{\max}$ for sandy clayey soils. The advantage of their approach, in comparison to that of Rollins et al. [7], is the facilitate estimation and interpretation of D values.

The cyclic deviator stresses, at earlier studies, were applied in uniform sinusoidal cycles at frequencies up to 0.2 Hz. The low frequency may be selected in order to measure the deformation accurately. ASTM D3999 [15] recommended a frequency variation between 0.1 and 2 Hz. Zhang et al. [9] indicated that there is a significant discrepancy at small strain levels between the recommended D curve and test data for $D_{\min}$ at different loading frequencies for sands. For example, by changing the frequency from 0.5 to 1 Hz at the confining pressure of 100 kPa, $D_{\min}$ increases from about 1% to about 5%. Similar values for high $D_{\min}$ have been reported by Lin et al. [8] on gravelly soils. Unfortunately, these researchers did not consider the effect of high frequency at low strains in their proposed $D - \gamma$ curve. Also, based on the back-calculated soil properties from vertical array records during the 1995 Kobe earthquake, Kokusho et al. [16] concluded that the damping ratio mechanism for strong ground motion is mostly hysteretic in nature and higher than expected.

Moreover, Khan et al. [17] have shown the dynamic properties of soils exhibiting strong visco-elastic behavior, which cannot be considered frequency independent in the earthquake frequency bandwidth (< 30 Hz [18]), even for low strain level excitations [12], as it is common practice in geotechnical engineering [19].

MATERIAL PROPERTIES

The tested gravelly samples were obtained from the shell and core materials of some earth and rock-fill dams under construction in Iran [20,21]. Table 1 summarizes the main characteristics of the materials

Table 1. Characteristics of gravelly materials used in large scale triaxial testing.

Material Name	Core/ Karkheh Dam	Core/ Vanyar Dam	Core/ Shahr-Chi Dam	Shell/Sattar Khan Dam	Shell/Zone 3B/MES	Shell/Zone 3A/MES	Shell/ Shahr-Chi Dam	Shell/ Sabalan Dam
Shape	Rounded to subrounded alluvium deposit	Subrounded to rounded alluvium deposit	Subangular to subrounded alluvium deposit	Rounded andesite & basalt	Angular limed conglomerated, weak cemented	Angular limed conglomerated, weak cemented	Rounded to subrounded alluvium deposit	Angular andesibasalt
Maximum In-Situ Particle Size (mm)	50	120	75	200	800	1000	150	400
Passing 4.75 mm	31	41	37	48	72	55	47	59
Passing 0.075 mm	49	30	31.8	14	13.8	6.5	11.1	0
PI	30	8.6	15.2	—	—	—	—	—
Gs	2.7	2.67	2.64	2.65	2.64	2.64	2.735	2.63
Dimension of Samples (cm)	20*40	20*40	20*40	30*60	30*60	30*60	30*60	30*60
e_o	0.476	0.283	0.276	0.335	0.28	0.281	0.227	0.223
95% ($\gamma_{\max}$) g/cm^3	1.83	2.08	2.03	2	2.177	2.121	2.19	2.11
W (%)	13.5	9.5	10.1	8.5	7.1	7.1	5.8	4.5
Loading Frequency (Hz)	1	1	1	1	0.1	0.1	1	1
Permeability (cm/s)	1*10e-7	2*10e-7	5*10e-7	1*10e-4	> 1*10e-3	> 1*10e-3	> 1*10e-0	> 1*10e-1
Material Symbol	C.K	C.V	C.SC	S.SK	S.3BMES	S.3AMES	S.SC	S.S

and some test conditions. The C.K was prepared from core materials used in the Karheh earthfill Dam. The material comprises rounded to subrounded alluvium deposits, which consist of 49% fines (< 0.075 mm) with Plasticity Index (PI) = 30%. The C.V material is the core material used for the Vanyar rockfill Dam. The materials are subrounded to rounded alluvium deposits and consist of 30% fines with a Plasticity Index of 8.6%. The C.SC was obtained from the core materials used for the Shahr-Chi earthfill Dam. The materials are subangular to subrounded alluvium deposits, which consist of 31.8% fines with PI = 15.2%.

In addition, it is worthwhile to mention that the S.SK Andesite and Basalt were prepared from shell materials used for the Sattar Khan earthfill Dam, which were collected from the riverbed at the dam site. Moreover the rock-fill materials (S.3BMES and S.3AMES) were produced by quarry blasting as was the S.S material. The individual particles are composed of Andebasalt and are very susceptible to particle breakage (Marsal's Breakage index - Bg [22] was estimated to be 5 at 300 kPa and 10 to 14 at 600-900 kPa of confining pressure). The above materials have been categorized into two groups: "with > 30% fine content" and "with < 15% fine content".

Maximum dry densities were estimated for all samples according to Modified Proctor, ASTM D1557 [23]. The percentage of fines (< 0.075 mm) varies from 0 to 49%; specific gravity (G_s) ranges from 2.63 to 2.73, and void ratio (e) varies from 0.22 to 0.47 for the tested materials.

Experimental Program

The gradation curves of the materials for triaxial testing were obtained using the parallel gradation modeling technique [24] with maximum particle sizes of 50 mm and 39 mm (1/6 and 1/5 diameter of the large-scale triaxial cell), as shown in Figure 1. The range of confining pressures was chosen with respect to the stress levels in the dams. Cyclic tests were conducted according to ASTM D 3999 [15]. These tests were conducted on large scale specimens with 200 and 300 mm diameters, and 400 and 600 mm heights under loading frequencies of 0.1 and 1 Hz. The tests on six different materials were carried out using the large-scale triaxial equipment of the Geotechnical Department of the Building and Housing Research Center (BHRC), Tehran, Iran. Also, another series of tests on Masjed-E-Soleyman rock-fill materials were carried out in Japan using similar equipment, but with a loading frequency of 0.1 Hz. In both series of tests, submersible

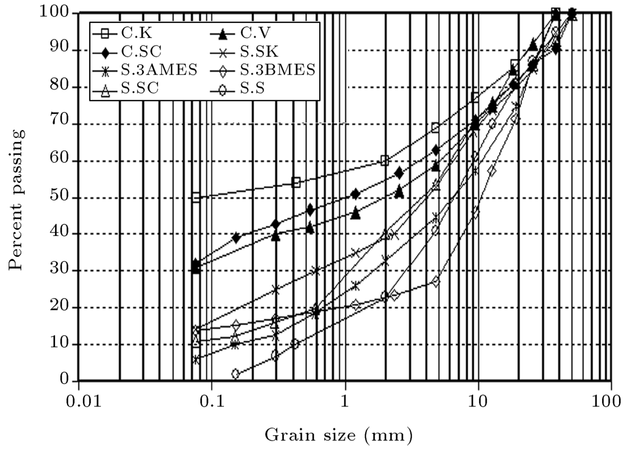

Figure 1. Grain size distribution for modeled rockfill materials in triaxial cyclic testing.

type load cells and a high sensitivity displacement transducer (non-contact type [25]) are located inside the cell pressure. Displacement sensors were typically placed on opposite sides of the top platen, so that the average strain could be determined and the rotational component eliminated. This approach excludes friction in the loading piston from loading measurements and enables accurate assessment of the shear strain to levels approaching 0.001%.

Testing Procedure

Specimens were compacted to 95% maximum dry density (according to Modified Proctor) in a split mold using a vibrator compactor operating at a frequency of 60 cycles/s. A silicone type membrane with a thickness of 2.5 mm is used to encase the specimen and provide reliable protection against leakage. Specimens were reconstituted in six layers. For each layer, the necessary quantity by weight of each granulometric class was mixed with the appropriate water content corresponding to 95% optimum density. After passing the CO_2 and applying a vacuum, the sample was partially saturated by allowing water to pass through the base of the triaxial cell and removing air bubbles. Also, in order to achieve full saturation (Skempton B greater than 95%), back-pressurization is used. Tests are performed under stress-control. The specimens were first subjected to the required consolidation pressures. Staged tests were performed to save cost and time. Initially, a limited number of cycles (i.e. 30 cycles), with desired loading frequency, were applied at a very small strain level. Only test result for cycles 11 to 23 have been recorded. The excess pore pressure developed during this cyclic loading was dissipated by opening the drainage valve so that the original effective stresses were regained. This procedure was then repeated at higher strain levels (about twice the initial amplitude) until the maximum strain level was achieved (> 0.7%). When the pore pressure was released by opening the drainage valve, the volume of the specimen decreased and, thus, the sample became a little denser. The change in volume depended on the axial strain amplitude, the number of strain cycles applied, and the sample type. It was found that the amount of change in density was negligible for small strain amplitudes, and was still very small even for strain amplitudes up to 0.1%, if the number of strain cycles was limited (see Figure 2). It is, therefore, believed that the re-use of samples for higher strain amplitudes still gives reasonably good results if the number of strain cycles applied is limited [1]. Axial loads, vertical displacements, volume changes and pore pressures were measured at periodic intervals of 0.02 seconds.

TEST RESULTS

Tests results including the shear modulus and damping ratio versus shear strains, are calculated based on the stress-strain hysteresis loop for the 11th cycle, according to ASTM D 3999[15]. Poisson's ratio, ν, is postulated as 0.5 in the present study because test spec-

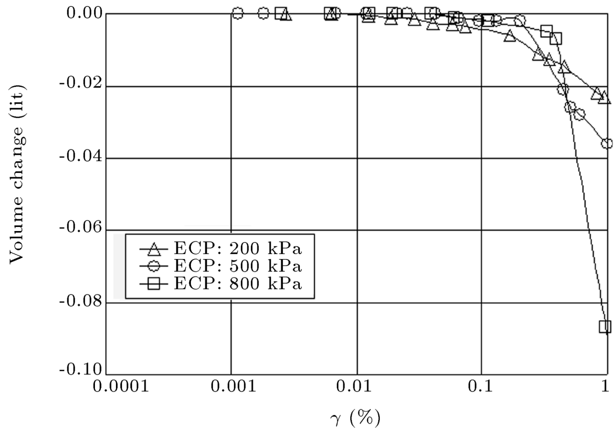

(a) C.SC

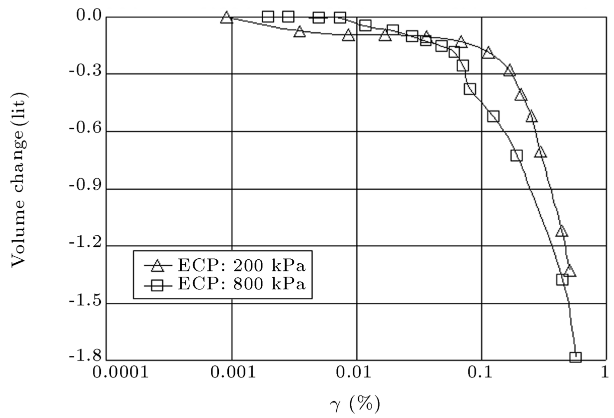

(b) S.SC

Figure 2. Volume change versus strain in gravelly materials [20].

imens are fully saturated and sheared under undrained conditions. A typical result of stress-strain hysteresis curves for C.SC and S.SC materials at the confining pressure of 800 kPa and at nearly the same strain level is presented in Figures 3a and 3b, respectively. As shown in Figure 3, the shape of the hysteresis curves for materials with > 30% fine content and materials with < 15% fine content have a significant difference at high strains. By comparison of Figure 3a with 3b, it can be concluded that the decrease in shear modulus with increasing strain for C.SC is more compared to S.SC. As indicated in Figure 3b, at higher strains, for S.SC, the values of the shear modulus are not constant and decrease with the number of cycles. This may be due to excess pore water pressure generation and, finally, degradation induced at high cyclic loading at S.SC with an increasing number of cycles of loading. But this phenomenon was not observed in C.SC, in which, with an increasing number of cycles, the amount of excess pore pressure generation is almost constant. Figure 4 presents the variation of excess pore water pressure generation in S.SC and C.SC at a confining pressure of 800 kPa. As shown in Figure 4, extra pore pressure may be responsible for further degradation of the shear modulus in S.SC material.

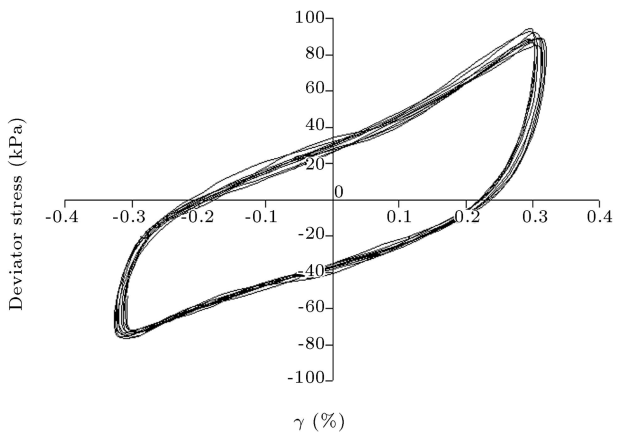

(a) C.SC

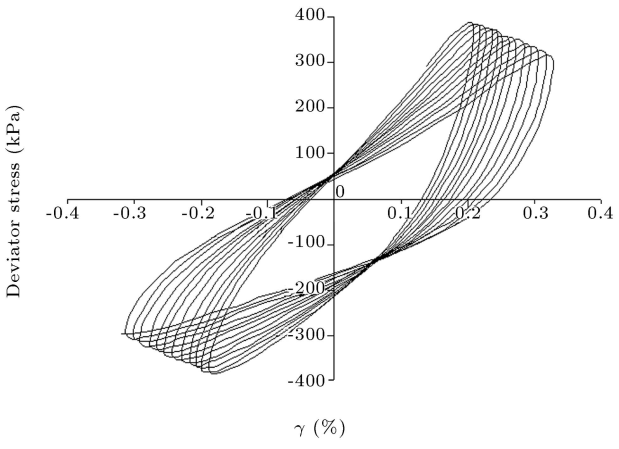

(b) S.SC

Figure 3. Hysteresis stress-strain loop in load control testing sample at confining pressure 800 kPa.

Figure 5 shows the variation of double amplitude excess pore water pressure versus shear strain in load control testing at different confining pressures in C.SC and S.SC; double amplitude excess pore water pressure in C.SC material first increases as confining pressure increases (up to 500 kPa) and finally decreases at higher confining pressure for the 11th cycle. However, for S.SC specimens, a continuous increase in excess pore pressure generation is observed with the number of cycles.

Shear Modulus

G versus γ data points for the materials under study are shown in Figure 6. As expected, with increasing confining pressure, G versus γ values increase.

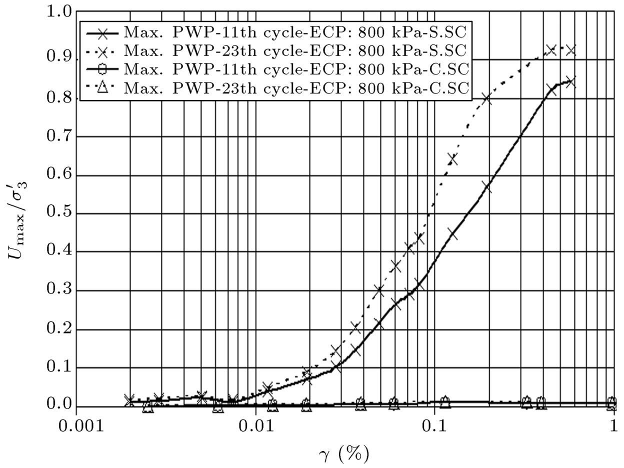

Figure 4. Excess pore water pressure generation in two gravelly materials at high confining pressure.

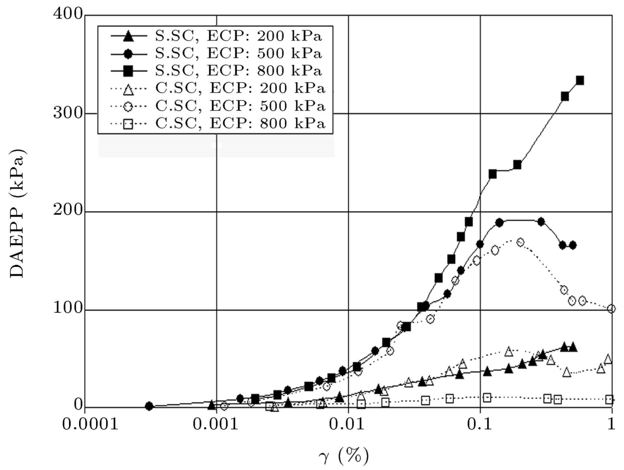

Figure 5. Variation of double amplitude excess pore water pressure at 11th cycle in load control testing for C.SC and S.SC.

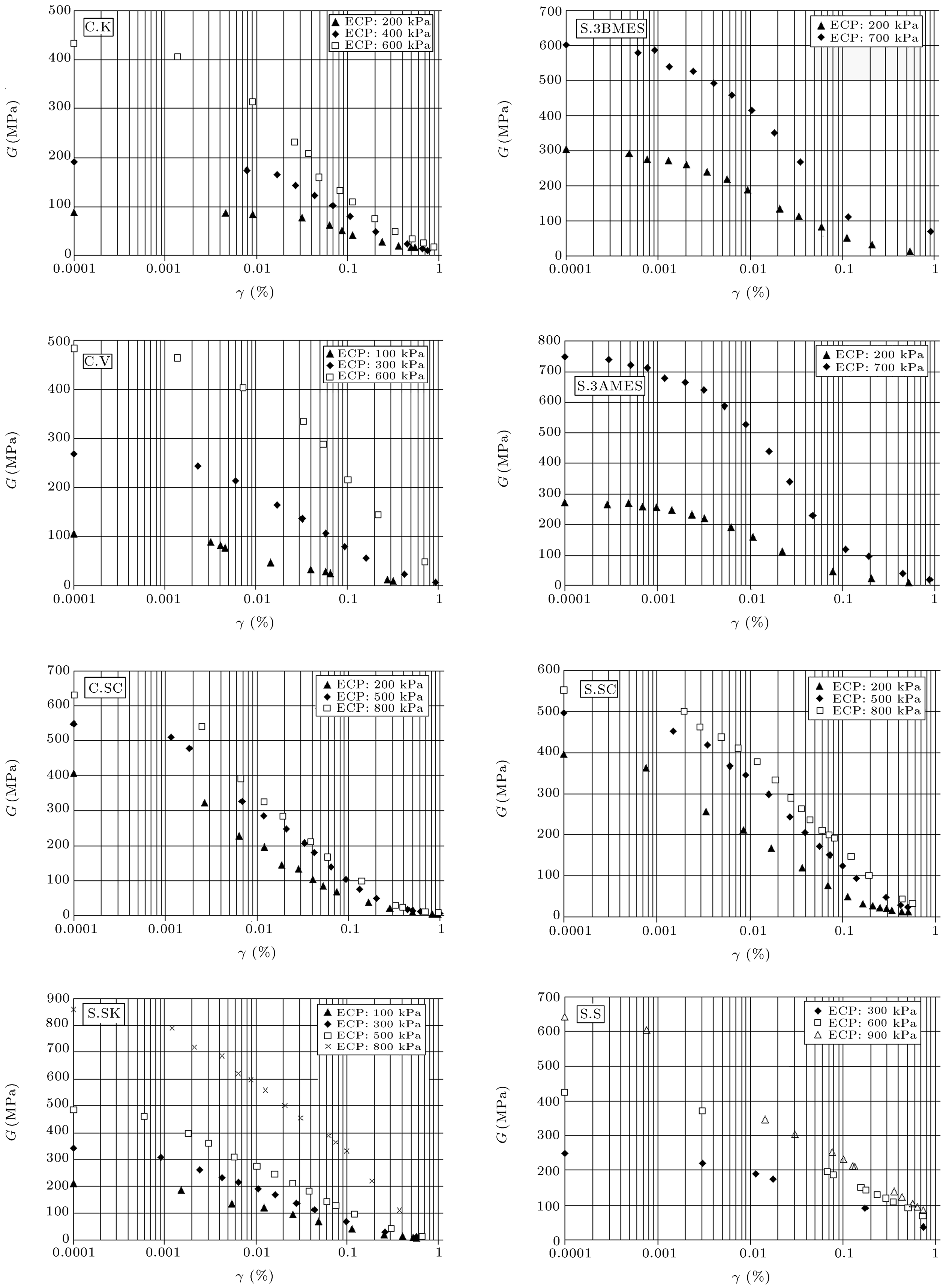

Figure 6. $G - \gamma$ relationship for different gravelly materials.

Low-Amplitude and Normalized Shear Modulus

Many researchers have attempted to develop equations for estimating $G_{\max}$. Seed et al. [1] employed the extrapolation method from the 0.0001% strain to obtain $G_{\max}$, which we employed also. In the present study, accurate monitoring of the strain was undertaken by means of non-contact type displacement transducers to infinitesimal strains as small as 0.001%. Since the strain level was still small in this type of test, there was no build-up of pore water pressure and samples were free from any deleterious effects due to membrane penetration. Values of $G_{\max}$ in this study have been presented in Table 2. The low-amplitude shear modulus of materials with 49% fine at given confining pressures has the lowest value.

$G/G_{\max}$ Relationships

$G/G_{\max}$ versus γ data points compiled for gravelly soils in this study is shown in Figure 7. The range of data for sands [11] and gravels [1] are also shown in Figure 7 for comparison. The Rollins et al. [7] $G/G_{\max} - \gamma$ curves for gravel are identical with the proposed curve for sand by Seed and Idriss [11], hence, for simplicity they are not presented in coming figures. Generally, as confining pressure increases, the mean curve moves from the lower bound toward the upper bound. There are two exceptions for C.K and S.S. The effects of confining pressures in C.V and S.SC are very clear. For S.SC material, as confining pressure increases, its effect on the values of $G/G_{\max}$ versus γ decreases; the variation of $G/G_{\max}$ from $\sigma'_3 = 200$ to 500 kPa is higher than from $\sigma'_3 = 500$ to 800 kPa. According to the results of this study, the variation of $G/G_{\max}$ versus γ at the frequency of 0.1 Hz lies within the ranges proposed by Seed et al. [1] (e.g. S.3AMES and S.3BMES), and confining pressure has minor effects on the $G/G_{\max}$ versus γ curve. Whereas the frequency of 1 Hz may be due to complex effects of fine content, high confining pressure, particle breakages, and especially loading frequency, some discrepancies with previous results were observed.

Table 2. Experimentally determined $G_{\max}$ of the tested materials.

Material	σ'_3 **(kPa)**	γ**(%) at** $G/G_{\max} = 0.5$	α	$(G/G_{\max})$ **measured =** $(G/G_{\max})$ **Calculated** (R^2)
C.K	200	0.10895	$\alpha = 1.8$ for $G/G_{\max} > 0.5$, $\alpha = 0.9$ for $G/G_{\max} < 0.5$	(0.985)
	400	0.0815		
	600	0.03615		
C.V	100	0.0117	$\alpha = 0.8$	(0.984)
	300	0.03735		
	600	0.0875		
S.SC	200	0.01125		
	500	0.0229		
	800	0.03385		
S.SK	100	0.02258		
	300	0.01855		
	500	0.01875		
	800	0.04395		
C.SC	200	0.0171	$\alpha = 0.9$	(0.99)
	500	0.0159		
	800	0.0173		
S.3BMES	200	0.01865		
	700	0.0267		
S.3AMES	200	0.0167		
	700	0.0235		
S.S	300	0.074	$\alpha = 0.6$	(0.987)
	600	0.06085		
	900	0.02965		
All data points of gravelly soils			$\alpha = 0.8$	(0.979)

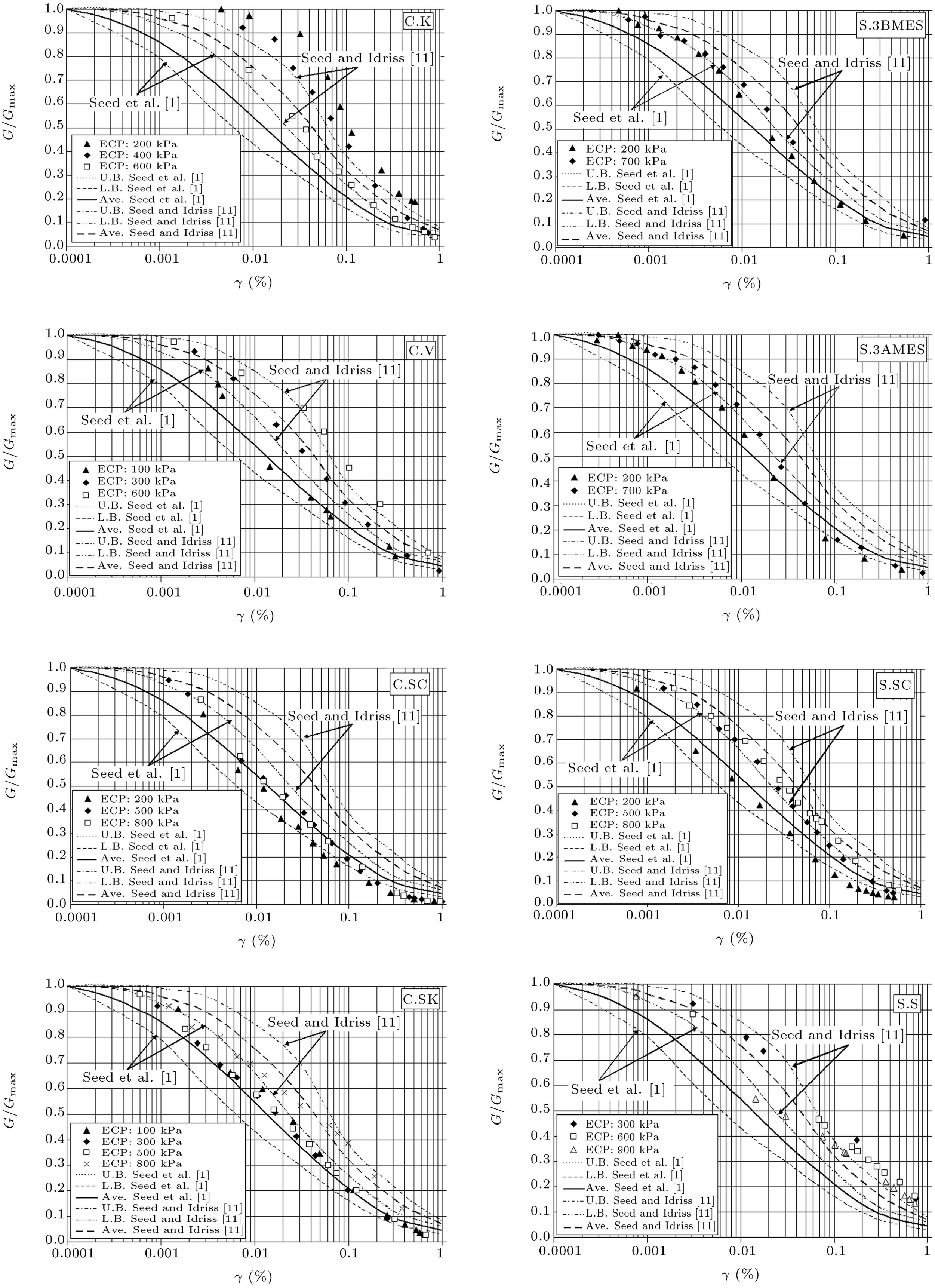

Figure 7. γ versus $G/G_{\max}$ relationship for gravelly materials. γ versus $G/G_{\max}$

Predictive Model for $G/G_{\max}$ Relationships

Hyperbolic models have widely been used to describe nonlinear soil behavior under cyclic loading [7,9,10,26-28]. The hyperbolic model used by [26] assumes that the stress-strain curve of a soil can be represented by a hyperbola, asymptotic to the maximum shear stress ($\tau_{\max}$). Since this model only involves a single curve-fitting variable, termed reference strain, it poorly fits test data. The modified hyperbolic model has been used for clayey soils [9,28]:

$$G/G_{\max} = 1/[1 + (\gamma/\gamma_r)^{\alpha}], \tag{1}$$

where γ_r is reference strain at $G/G_{\max} = 0.5$ and α is the second curve-fitting variable called the curvature parameter. The above model has been used for coarse grain soils at different σ'_3. Values of α and γ_r that provide best fits for Equation 1 for the compiled test data are determined by multiple regression. Computed values of γ_r and, α at different σ'_3 for the materials of this study are presented in Table 3.

Figure 8 compared the calculated values of $G/G_{\max}$ (Equation 1) with the measured values for S.3BMES and S.SC. Good agreement between tests results and corresponding modeling results is evident, indicating that the hyperbolic model is capable of capturing the behavior of the rock-fill materials. These results are typical. Favorable results were obtained for the other rock-fill type specimens.

Calculated values of $G/G_{\max}$ are compared with measured values for all materials in this study and presented in Figure 9. The plotted data points distribute evenly around the "measured = calculated" line, with coefficient of correlation (R^2) values ranging from 0.979 to 0.99 for different materials. When interpreting the R^2 values, one point to keep in mind is that the $G/G_{\max}$ data around 0.5 have inherently small errors because of normalization. As a result, the R^2 values completely reflect the goodness-of-fit of the recommended model.

Damping Ratio

D versus γ data points for the materials under study are shown in Figure 10. The trend lines established by Seed et al. [1] and Rollins et al. [7] for sands and gravels are also shown in Figure 10 for comparison. Interestingly, the damping ratios of the gravelly soils

Table 3. σ'_3, γ_r and α for the gravelly materials.

Material	**γ(%) at $G/G_{\max} = 0.5$**	**σ'_3 (kPa)**	**α**	**($G/G_{\max}$) Measured = ($G/G_{\max}$) Calculated (R^2)**
C.K	0.10895	200	$\alpha = 1.8$ for $G/G_{\max} > 0.5$, $\alpha = 0.9$ for $G/G_{\max} < 0.5$	(0.985)
	0.0815	400		
	0.03615	600		
C.V	0.0117	100	$\alpha = 0.8$	(0.984)
	0.03735	300		
	0.0875	600		
S.SC	0.01125	200		
	0.0229	500		
	0.03385	800		
S.SK	0.02258	100		
	0.01855	300		
	0.01875	500		
	0.04395	800		
C.SC	0.0171	200	$\alpha = 0.9$	(0.99)
	0.0159	500		
	0.0173	800		
S.3BMES	0.01865	200		
	0.0267	700		
S.3AMES	0.0167	200		
	0.0235	700		
S.S	0.074	300	$\alpha = 0.6$	(0.987)
	0.06085	600		
	0.02965	900		
All data points of gravelly soils			$\alpha = 0.8$	(0.979)

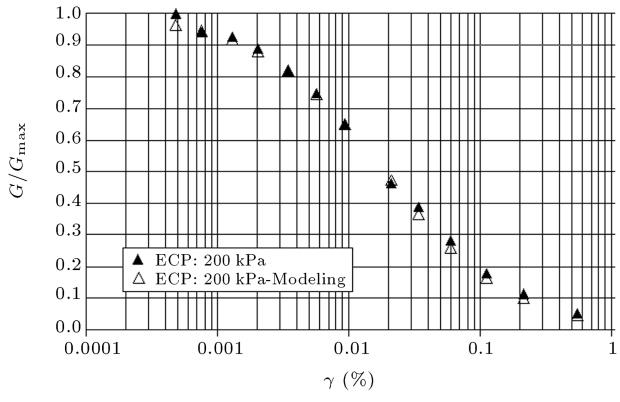

(a) S.3BMES

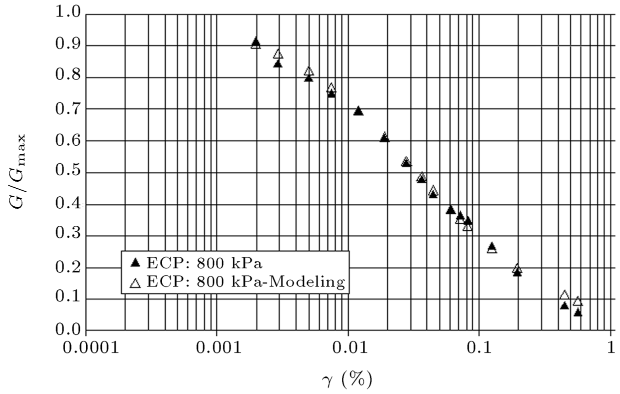

(b) S.SC

Figure 8. Comparison of measured and calculated $G/G_{\max}$ for two gravelly materials.

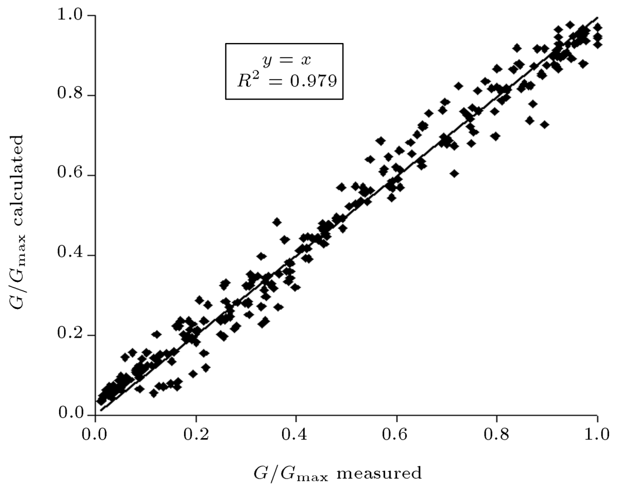

Figure 9. Comparison of measured and calculated $G/G_{\max}$ for gravelly materials.

are slightly affected by confining pressures and fall within a narrow band. This phenomenon may be due to sample preparation at maximum dry density. There is an exception for the damping ratio of C.K samples with increasing confining pressure. It may be attributed to the positive effect of coarse grain content and less pore pressure generation due to high consolidation (lower void ratio at higher confining pressure) in the specimens (Figure 10).

Most damping ratio data of gravelly materials at 0.04% to 0.5% strain levels follow the range identified by Seed et al. [1]. However, this phenomenon was not clearly evident in the S.S sample in which damping ratios are restricted within a small bound for all strains and confining pressures. As noted before, the S.S materials are very susceptible to particle breakage especially at high confining pressures. Similar behavior is reported by Seed et al. [7] for weak Venado sandstone, the damping ratios of which fall within a small bound for all densities. Damping ratios below 0.04% strain do not follow the trend as observed by Seed et al. [7]. However, as indicated in Figure 10, D versus γ data points for S.3AMES and S.3BMES materials tested at 0.1Hz fall within ranges proposed by previous researchers.

COMPARISON OF RESULTS WITH PREVIOUS STUDIES

The Seed et al. [1] and Rollins et al. [7] curves are primarily based on specimens at low stress levels ($<$ 490 kPa) and low loading frequency. The compiled data and the recommended $G/G_{\max}$ and D versus γ curves for gravelly soils of earth-rock-fill dams (with $>$ 30% fine content and with $<$ 15% fine content) are compared with the Seed et al. [1], Seed and Idriss [11] and Rollins et al. [7] curves in Figures 11 and 12, respectively. The Seed and Idriss [11] $G/G_{\max} - \gamma$ curves for sand are identical with the proposed curves for gravel by Rollins et al. [1] and which, hence for simplicity, are not presented in these figures. Figure 11a indicates that the $G/G_{\max}$ value of materials with $<$ 15% fine content approximately fall within the ranges proposed by Seed et al. [1] and Rollins et al. [7]; it seems that the lower bound of Seed et al. [1] and the upper bound of Rollins et al. [7] curves are appropriate curves, but need some modification at the upper bounds of Rollins et al. [7]. Comparing Figures 11a and 11b reveals that with increasing fine content, there are significant differences between the proposed curves; and materials with $>$ 30% fine content have a more elastic range at low strains. The data in these figures clearly indicate a need for the modification of previously proposed curves, particularly for gravels with high fine content.

Figure 12a presents the D versus γ data for materials with $<$ 15% fine content together with those of Seed et al. [1] and Rollins et al. [7]; at high strain, data lie completely above the main proposed curve by Rollins et al. [7], whereas at low strain a considerable amount of the data lie above the upper bound proposed by Seed et al. [1]. Figure 12b shows the recommended D versus γ for materials with $>$ 30% fine content of the present study, together with those of Seed et al. [1]

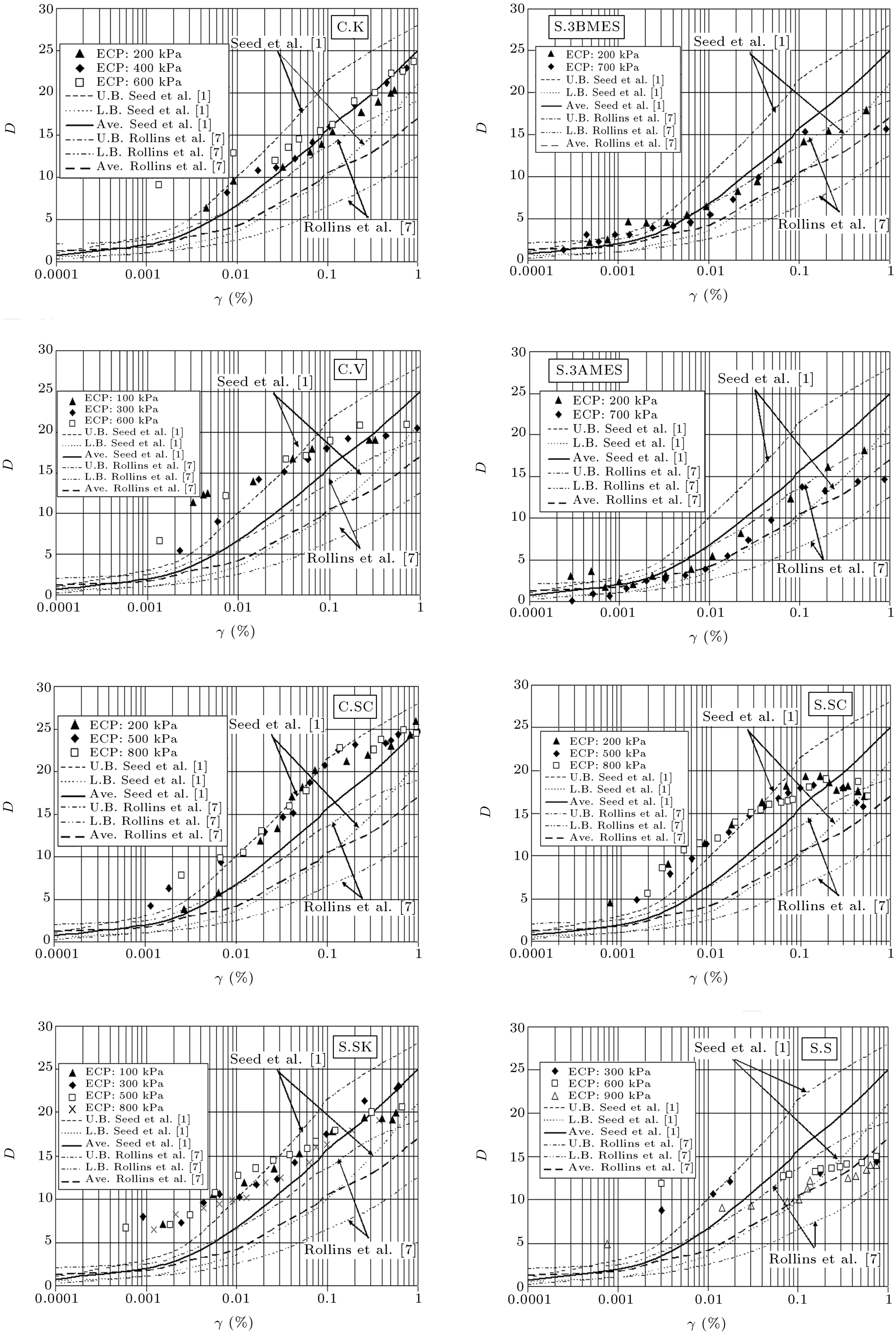

Figure 10. $D-\gamma$ relationship for different materials.

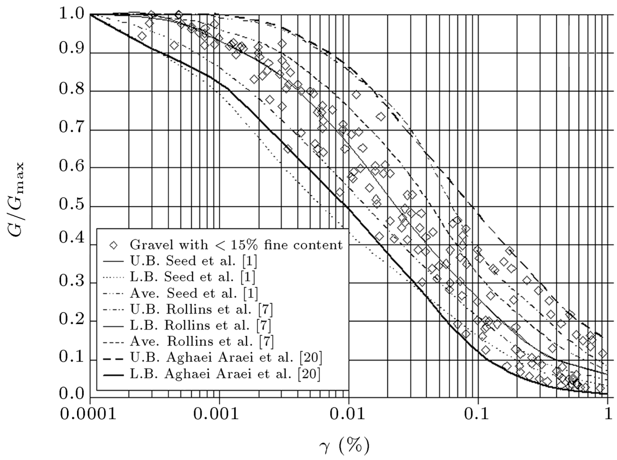

(a)

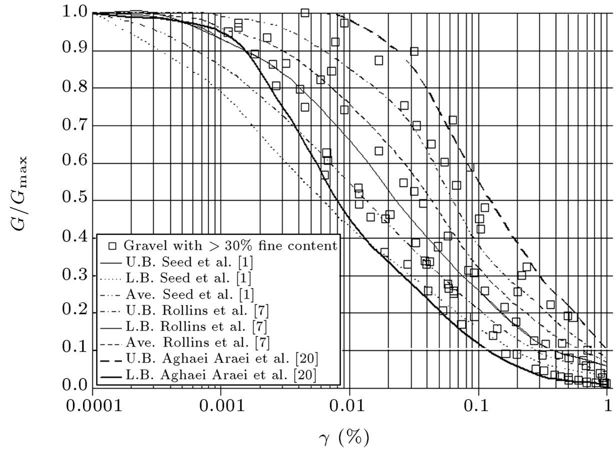

(b)

Figure 11. $G/G_{\max}$ versus γ relationship for gravelly soils based on this study. (a) $<15\%$ fine content. (b) $>30\%$ fine content (curves defining range of data for gravels [1,7] shown for comparison).

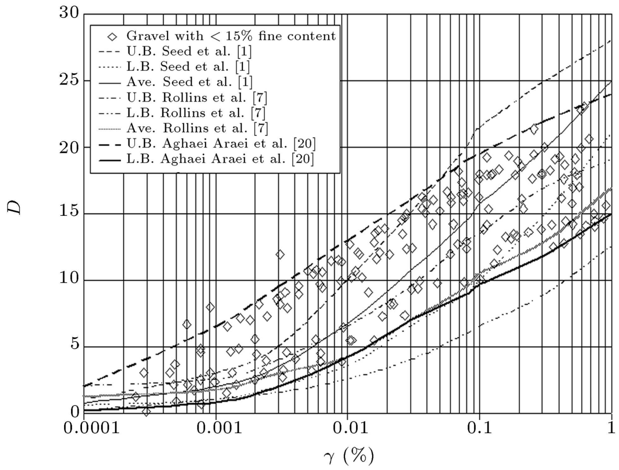

(a)

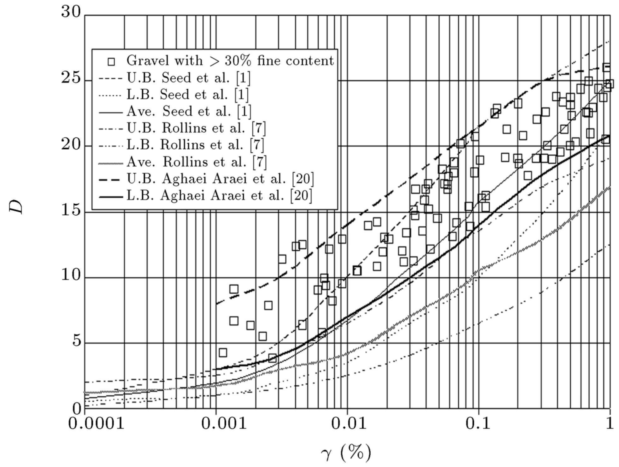

(b)

Figure 12. D versus γ relationship for gravelly soils based on this study. (a) $<15\%$ fine content. (b) $>30\%$ fine content (curves defining range of data for gravels [1,7] shown for comparison).

and Rollins et al. [7]. Figure 12b indicates that the D versus γ data for materials with $>30\%$ fine content lie completely above the upper bound proposed curve by Rollins et al. [7]. It is observed that a considerable number of the present study's data points fall outside the ranges proposed by researchers, especially at low strains. Comparing Figures 12a and 12b suggests that in gravelly materials, as fine content increases, the damping ratio increases at high strain (nearly 1%). The high values of damping at low strains for study materials with a low void ratio ($e < 0.5$) may be attributed to the sensitivity of their structure to loading frequency; the increased interaction of soil particles results in a high dissipation of energy at particle contact [29]. Aghaei Araei et al. [30] also investigated loading frequency effects on the damping properties of high compacted rock-fill material. The data presented in Figure 13 indicated that in all ranges

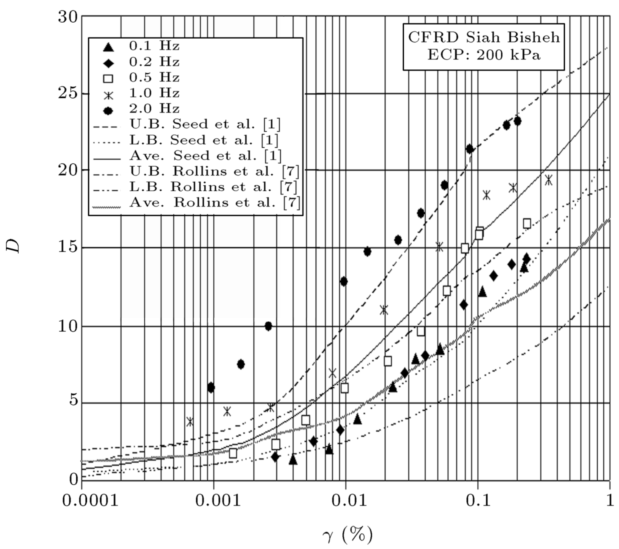

Figure 13. Effects of frequency content on dynamic properties of gravelly soils [30].

of the strains investigated, damping ratios increase as loading frequency increases.

$G/G_{\max}$ AND D RELATIONSHIPS

There are some discrepancies between $G/G_{\max} - \gamma$ and $D - \gamma$ curves proposed by Seed et al. [1] and Rollins et al. [7] with the results of this study for gravels especially at low shear strain, which may be due to more fine content and loading frequency. The modulus reduction equation originally developed by Zhang et al. [9] for sands, silts and clays have been expanded to include gravelly soils. The general damping equation adopted for this study is:

$$D = A(G/G_{\max})^3 + B(G/G_{\max})^2 + C(G/G_{\max}) + D_{\max}, \tag{2}$$

where A, B and C are constants. Table 4 and Figure 14 presented $D_{\max}$, D and $G/G_{\max}$ relationships for development of the best-fit according to Equation 2. The main curves defining the range of data for gravels [1,7] are shown for comparison.

Figure 14a compares the main curves of Seed et al. [1] and Rollins et al. [7] with the results from S.3AMES and S.3BMES. This figure shows that good agreement exists between the test data and curve proposed by Rollins et al. [7] especially at low to medium strains. This may be due to the same applied loading frequency, whereas for the remaining material, a considerable amount of data is above the proposed curves by Seed et al. [1] and Rollins et al. [7], which may be due to the complex effect of loading frequency, high fine content and high confining pressure.

As shown in Figure 14a, D versus $G/G_{\max}$ curves for S.3AMES, S.3BMES and S.SK are independent of confining pressures. As indicated in Figure 14a, the difference between S.SK and S.3BMES with equal fine content may be due to the complex effects of loading frequency and different maximum particle size;

Table 4. $D - G/G_{\max}$ relationship.

σ'_3 (kPa)	Material	$D = A(G/G_{\max})^3 + B(G/G_{\max})^2 + C(G/G_{\max}) + D_{\max}$				(R^2)
		A	B	C	$D_{\max}$	
200						
400	C.K	-31.74	55.637	-41.995	25.259	0.9626
600						
100						
300	C.V	-12.521	8.9768	-10.356	20.715	0.8273
600						
200						
500	C.SC	14.317	-8.2661	-25.119	24.956	0.9811
800						
100						
300	S.SK	2.7044	-0.0904	-17.856	24.97	0.9919
500						
800						
200	S.3BMES	-8.2116	22.318	-31.207	19.215	0.9807
700						
200	S.3AMES	-0.403	10.8	-25.707	16.948	0.972
700						
200						
500	S.SC	8.6732	-29.332	6.9232	17.508	0.9308
800						
300						
600	S.S	-47.758	70.565	-33.651	18.625	0.815
900		-12.309	23.647	-23.949	16.894	0.9684
Average Rollins et al. [7]		-20.022	39.902	- 37.792	19.08	0.9954
Average Seed et al. [1]		-23.216	60.227	- 63.076	26.715	0.9952
Materials with > 30% fine content		-20.535	39.229	-36.378	24.781	0.8794
Materials with < 15% fine content		-15.852	18.392	-19.664	19.07	0.7875
All gravelly materials		-23.178	35.44	-30.988	21.969	0.7674

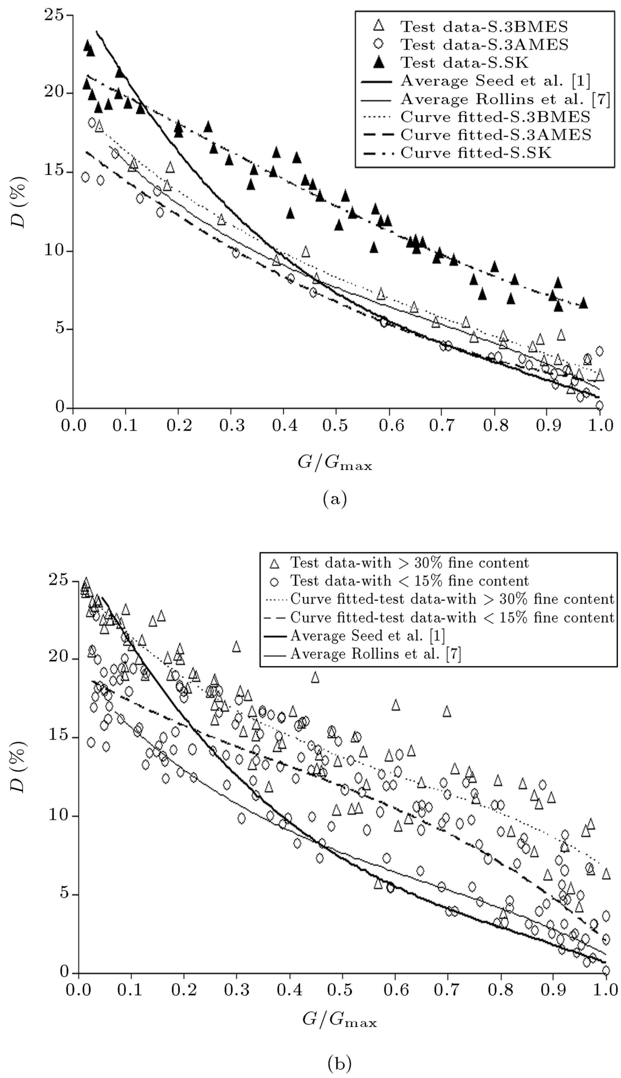

Figure 14. $D - G/G_{\max}$ relationships.

loading frequency seems to be more responsible for the difference.

As shown in Figure 14b, it seems that D is sensitive to fine content, which may be due to the fact that fine materials play the role of lubricant between coarse grains, easing the slipping of coarse grains, and as a result, the values of D increase.

EFFECT OF NUMBER OF CYCLES ON DYNAMIC PROPERTIES OF GRAVELLY SOILS

Essentially, in cyclic loading, according to ASTM D 3999 [15], it is assumed that after applying 10 cycles, the degradation should be eliminated and in coming cycles, G and D are measured under a steady state condition. However, it was observed that both G and σ'_3 varied to some extent with increasing the number of cycles for each strain amplitude [1].

In this study, test results including effects of the number of cycles on G value (i.e. G_{11}/G_{20}) versus shear strain are summarized in Table 5. For comparison purposes, it was considered that the most appropriate G was the modulus G at the 11th cycle, since this is considered a representative average for many earthquakes in Iran. Generally, the values of G_{11}/G_{20} increased at strain between 0.01% and 0.5%. Table 5 indicated that for C.K (with 49% fine content), and $G_{11}/G_{20} = 1.2$ at $\gamma = 0.5\%$. For S.SC (containing 12% fine content), the corresponding value is 1.55 at $\gamma = 0.35\%$, and for C.V. is 1.45 at $\gamma = 0.5\%$. After the mentioned strain, the value of G_{11}/G_{20} reached to 1. The value of G_{11}/G_{20} of S.S is always higher than 1 and increases at a shear strain higher than 0.01% markedly.

Table 5. Effect of number of cycles on G_{11}/G_{20} results versus shear strains.

Materials	**Threshold Shear Strain with $G_{11}/G_{20} > 1$**	**Shear Strain at max. G_{11}/G_{20} (Left Column) and Its Value (Right Column)**		**Final Shear Strain (%) (Left Column) and G_{11}/G_{20} Value (Right Column)**	
C.K	0.04	0.5	1.2	1	1
C.V	0.03	0.5	1.45	1	1
C.SC	0.03	0.5	1.15	1	1
S.SK	0.01	0.4	1.35	0.7	1.1
S.SC	0.01	0.35	1.55	0.6	1.3
S.S	0.01	0.8	1.3	0.8	1.3
Material with > 30% fine content	0.03	0.5	1.25	1	1
Material with < 15% fine content	0.01	0.4	1.4	0.75	1.15
All gravelly materials	0.02	0.45	1.32	0.9	1.08

Generally, the average values of G_{11}/G_{20} of material with $> 30\%$ fine content (at $\gamma = 0.5\%$), material with $< 15\%$ fine content (γ=0.4%) and all materials ($\gamma = 0.45\%$) are 1.25, 1.4 and 1.32, respectively (Figure 15, Table 5). It must be noted that at shear strain higher than about 0.5%, the G_{11}/G_{20} value reached to 1. However, the number of cycles does not affect the general trend of $G - \gamma$ curves especially at low strains; the case of S.S is an exception. Conversely, it seems that D results were not significantly affected by the number of cycles (in the studied cycle number) for gravelly materials (for example see Figure 16).

CONCLUSIONS

Triaxial testing results and predictive equations for estimating the normalized shear modulus and damping ratio of some gravelly soils are presented in this study. The tests on modeled gravelly soils are carried out with large scale triaxial equipment. Based on the studies described in the preceding pages, it may be concluded that:

- Fine content of gravelly soils has some effect on G and D values. The average D value in materials with $> 30\%$ fine content is more than that of those with $< 15\%$ fine content.
- Data presented in this study clearly show the need for the modification of previous proposed curves for $G/G_{\max}$ and D versus γ, especially for gravel materials with fine content more than 30%.
- Damping ratios of gravelly material are slightly confining pressure, dependent of confining pressure. This may be due to sample preparation at maximum dry density.
- Damping ratios of gravel materials were somewhat higher at low shear strains in comparison with previously proposed ranges. This may be due to a higher loading frequency and more fine content in comparison with previous ones. For the studied materials, low void ratio and loading frequency may be responsible for higher damping ratios at low strains.
- Presentation $G/G_{\max} - D$ curves of gravelly soils may cause an easier interpretation of the complex effects of fine content, confining pressure and testing frequency.
- The number of cyclic loadings has a slight effect on G results, especially at shear strain more than 0.01%, for gravelly materials with low fine content ($< 15\%$), due to excess pore pressure generation.
- Loading frequency has some effect on D results; increasing loading frequency causes higher damping ratio, but increasing G with increasing loading frequency is negligible.
- Based on two later results, it is suggested that G and D should be measured at the number of cyclic loadings and frequency, similar to those of the anticipated cyclic loading to account for corresponding effects.

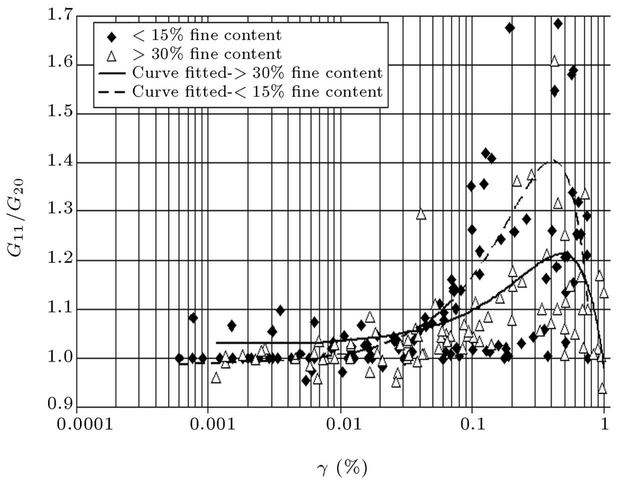

Figure 15. Effect of number of cycles on G_{11}/G_{20} results versus shear strains of gravelly materials.

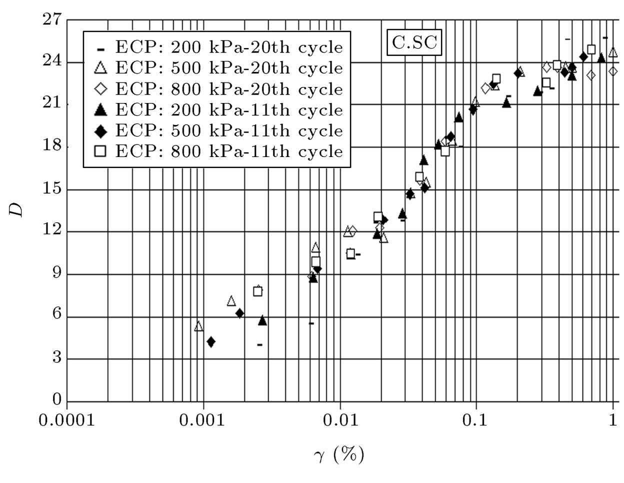

Figure 16. Effect of number of cycles on D versus shear strains for C.SC materials.

ACKNOWLEDGMENT

This material is based upon work supported by BHRC under grants No. 3-4469(2007) and 1-1775(2008). The authors are also thankful to the Iran Water Resources and Development Company, as the first projects' client, for financial aid and providing data for this research. The first author is thankful for the technical help given by his colleagues at the Geotechnical Division of BHRC. Also, the authors wish to thank the reviewers and referees of this paper for their constructive comments and valuable suggestions.

NOMENCLATURE

ν	Poisson's ratio
σ_3'	effective confining pressure
Ave.	average
B_g	Marsal's breakage index
D	damping ratio
D_{11}	damping ratio at 11th cycle
D_{20}	damping ratio at 20th cycle
DAEPP	Double Amplitude Excess Pore Pressure
D_r	relative density
ECP	Effective Confining Pressure
e_i	void ratio at end of consolidation
e_o	void ratio according to modified proctor compaction
$G/G_{\max}$	normalized shear modulus
G	shear modulus
G_{11}	modulus G at 11th cycle
G_{20}	modulus G at 20th cycle
$G_{\max}$	maximum value of shear modulus
G_s	specific gravity
Hz	Hertz
L.B.	Lower Bound
Max PWP 11th cycle	accumulated pore water pressure at the end of the 11th cycle
Max PWP 23rd cycle	accumulated pore water pressure at the end of the 23rd cycle
PI	Plasticity Index
R^2	coefficient of correlation
U.B.	upper bound
W_{opt}	optimum water content
γ	shear strain
γ_d	dry density
γ_r	reference strain at $G/G_{\max} = 0.5$

REFERENCES

1. Seed, H.B., Wong, R.T., Idriss, I.M. and Tokimatsu, K. "Moduli and damping factors for dynamic analyses of cohesionless soils", *J. Geotech. Eng.*, **112**(11), pp. 1016-1032 (1986).
2. Shibuya, S., Kong, X.J. and Tatsuoka, F. "Deformation characteristics of gravels subjected to monotonic and cyclic loading", in *Proceedings of the 8th Japan Earthquake Engineering Symposium*, **1**, pp. 771-776 (1990).
3. Goto, S., Nishio, S. and Yoshimi, Y., *Dynamic Properties of Gravels Sampled by Ground Freezing: In Ground Failure Under Seismic Conditions*, S. Prakash and P. Dakoulas, Eds., ASCE Geotechnical Special Publication No. 44, pp. 141-157 (1994).
4. Kokusho, T. and Tanaka, Y., *Dynamic Properties of Gravel Layers Investigated by In-Situ Freezing Sampling: In Ground Failure Under Seismic Conditions*, S. Prakash and P. Dakoulas, Eds., ASCE Geotechnical Special Publication No. 44, pp. 121-140 (1994).
5. Yasuda, N. and Matsumoto, N. "Comparisons of deformation characteristics of rockfill materials using monotonic and cyclic loading laboratory tests and in situ tests", *Canadian Geotechnical Journal*, **31**, pp. 162-174 (1994).
6. Hatanaka, M. and Vchida, A. "Effects of test methods on the cyclic deformation characteristics of high quality undisturbed gravel samples", *Static and Dynamic Properties of Gravelly Soils*, Geotechnical Special Publication No. 56, pp. 136-151 (1995).
7. Rollins, K.M., Evans, M.D., Diehl, N.B. and Daily, W.D. "Shear modulus and damping relationships for gravels", *Journal of Geotechnical and Geoenvironmental Engineering, ASCE*, **124**(5), pp. 398-405 (1998).
8. Lin, S., Lin, P.S., Luo, H. and Juang, H. "Shear modulus and damping ratio characteristics of gravelly deposits", *Canadian Geotechnical Journal*, **37**, pp. 638-651 (2000).
9. Zhang, J., Andrus, R. and Juang, C.H. "Normalized shear modulus and material damping ratio relationships", *Journal of Geotechnical and Geoenvironmental Engineering, ASEC*, **4**, pp. 453-464 (2005).
10. Hardin, B. and Kalinski, M. "Estimating the shear modulus of gravelly soils", *Journal of Geotechnical and Geoenvironmental Engineering, ASEC*, **7**, pp. 867-875 (2005).
11. Seed, H.B. and Idriss, I.M. "Soil moduli and damping factors for dynamic analysis", Report No. EERC 70-10, University of California, Berkeley (1970).
12. Lai, C.G., Pallara, O., Lo Presti, D.C. and Turco, E. "Low-strain stiffness and material damping ratio coupling in soils; advanced laboratory stress-strain testing of geomaterials", T. Tatsuoka, S. Shibuya, and R. Kuwano, Eds., Balkema, Lisse, The Netherlands, pp. 265-274 (2001).
13. Darendeli, M.B. "Development of a new family of normalized modulus reduction and material damping curves", PhD dissertation, Univ. of Texas at Austin, Austin, Tex. (2001).
14. Stokoe, K.H., II, Darendeli, M.B., Gilbert, R.B., Menq, F.Y. and Choi, W.K. "Development of a new family of normalized modulus reduction and material damping curves", Proc., NSF/PEER Int. Workshop on Uncertainties in Nonlinear Soil Properties and their Impact on Modeling Dynamic Soil Response, Univ. of California at Berkeley, Berkeley, Calf. (2004), http://peer.berkeley.edu/lifelines/workshop304/
15. Standard Test Methods for the Determination of the Modulus and Damping Properties of Soils Using the Cyclic Triaxial Apparatus, ASTM D3999 - 91(2003).
16. Kokusho, T., Aoyagi, T. and Wakunami, A. "In-situ soil-specific nonlinear properties back-calculated from

vertical array records during 1995 Kobe earthquake", *Journal of Geotechnical and Geoenvironmental Engineering, ASCE*, **131**(11), pp. 1509-1521 (2005).

17. Khan, Z.H., Cascante, G., El Naggar, M.H. and Lai, C.G. "Measurement of frequency-dependent dynamic properties of soils using the resonant-column device", *Journal of Geotechnical and Geoenvironmental Engineering, ASCE*, **134**(9), pp. 1319-1326 (2008).
18. Meng, J. "Earthquake ground motion simulation with frequency-dependent soil properties", *Soil Dynamics and Earthquake Engineering, Elsevier*, **27**, pp. 234-241 (2007).
19. Shibuya, S. and Mitachi, T. "Strain-rate effects on shear modulus and damping of normally consolidated clay", *Geotech. Test J.*, **18**(3), pp. 365-375 (1995).
20. Aghaei-Araei, A., Tabatabaei, S.H. and Ghalandarzadeh, A. "Assessment of shear modulus and damping ratio of gravelly soils", *Research Project*, No. 3-4469- 2007, BHRC, Iran (2008).
21. Aghaei Araei, A., Soroush, A. and Rayhani, M.H.T. "Large-scale triaxial testing and numerical modeling of rounded and angular rockfill materials", *Scientia Iranica, Trans. A, Civil Eng.*, pp. 169-83 (2010).
22. Marsal, R.J. "Large scale testing of rockfill materials", *Journal of the Soil Mechanics and Foundations Division, ASCE*, **93**(SM2), pp. 27-43 (1967).
23. *Standard Test Methods for Laboratory Compaction Characteristics of Soil Using Modified Effort*, ASTM D1557 (2007).
24. Lowe, J. "Shear strength of coarse embankment dam materials", *Proc., 8th Int. Congress on Large Dams*, **3**, pp. 745-761 (1964).
25. Kokusho, T. "Cyclic triaxial test of dynamic soil properties for wide strain range", *Soils and Foundations*, **20**, pp. 45-60 (1980).
26. Hardin, B.O. and Drnevich, V.P. "Shear modulus and damping ratio in soils: Measurement and parameter effects", *J. Soil Mech. and Foundation. Div., ASCE*, **98**, SM6, pp. 603-624 (1972a).
27. Pyke, R.M. "Modeling of dynamic soil properties, guideline for determining design bases ground motions", *Appendix 7.A, Electric Power Research Institute, 7.A-1-7, A-90* (1993).
28. Stokoe, K.H., II, Darendeli, M.B., Andrus, R.D. and Brown, L.T. "Dynamic soil properties; laboratory, field and correlation studies", *Proc., 2nd Int. Conf. on Earthquake Geotechnical Engineering*, **3**, Lisbon, Portugal, pp. 811-845 (1999).
29. Kallioglou, P., Tika, T.H. and Pitilakis, K. "Shear modulus and damping ratio of cohesive soils", *Journal of Earthquake Engineering*, **12**, pp. 879-913 (2008).
30. Aghaei-Araei, A., Razeghi, H.R., Tabatabaei, S.H. and Ghalandarzadeh, A. "Evaluation of frequency content on properties of gravelly soils", *Research Project*,No.1-1775-2008, BHRC, Iran (2009).

BIOGRAPHIES

Ata Aghaei Araei is a PhD candidate in the School of Civil Engineering at the Iran University of Science and Technology (IUST) and also PhD Researcher at the Geotechnical Laboratory of Civil Engineering at The University of Tokyo. Since 2003, he has been working as Senior Geotechnical Engineer and Head of the Geotechnical Laboratory at the Building and Housing Research Center (BHRC). Mr. Aghaei-Araei's primary research interests include: Monotonic and Dynamic Testing on Geomaterials, Microzonation, Geotechnical Equipment Construction.

Hamid Reza Rezeghi received his PhD from Tohoku University, Japan, in 2000 and is now an Assistant Professor in the School of Civil Engineering at the Iran University of Science and Technology, in Iran. His research interests include: Geotechnical and Geoenvironmental Engineering.

Saeid Hashemi Tabatabaei received his PhD from Roorkee University, India, in 1992. He is a faculty member of the Building and Housing Research Center (BHRC) in Iran where, since 2002, he has been Head of the Geotechnical Department. He has over 18 years experience in the field of geotechnical engineering and geotechnical engineering research. He has been involved in over 33 engineering projects in the fields of Landslide Hazard and Risk Assessment, Slope Stability Analysis and Mitigation, Soil Improvement, Engineering Geological Mapping for Microzonation of Rural Areas and Site Investigation.

Abbas Ghalandarzadeh is Assistant Professor in the School of Civil Engineering at the University of Tehran, where he is also currently Head of the Soil Mechanics and Centrifuge Laboratory. He received his PhD degree in Geotechnical Engineering from the University of Tokyo in 1997. He is a member of the Technical Committee of TC2 of the International Society of Soil Mechanics and Geotechnical Engineering. His research interests are mainly in the area of Experimental Geotechnics, particularly in model and element testing. Dr. Ghalandarzadeh has undertaken much research in the area of Earthquake Geotechnical Engineering including specifically: the Dynamic Behavior of Rockfill Dams with Asphalt Concrete Cores, the Seismic Behavior of Quay Walls, Reinforced Earth and Piles, and more recently the Anisotropic Behavior of Saturated Sands Mixed with Clay or Silt.